Simulation of Air Pad Shape on Pressure Distribution in Air Gap of Air Table in Ultra Precision Machine Tools

M. Akhondzadeh*
Department of Mechanical Engineering,
Islamic Azad University, Ahvaz branch, Khuzestan, Iran
E-mail: m_akhondzadeh@iauahvaz.ac.ir
*Corresponding author

M. Vahdati
Department of Mechanical Engineering,
K. N. Toosi University of Technology, Tehran, Iran
E-mail: Vahdati@kntu.ac.ir

Received: 24 April 2012, Revised: 15 October 2012, Accepted: 14 January 2013

Abstract: Air pads are vastly applicable in ultra precision machines. Spindle and table are the two main components of these machines which get advantages of such systems. The performance and efficiency of air pads have big influence on the whole machine quality. Parameters affecting pressure distribution of air tables may be considered as, 1) air compressing method, 2) air nozzle diameter, shape, and size, 3) number of air pads, and 4) air gap thickness. In this study, effects of air pad shape on pressure distribution in air gap have been investigated using ANSYS. In this simulation, FOTRAN environment have been employed. Investigated shapes for air pads are triangle, rectangle, pentagon, hexagon, ellipse and circle. Pressure distribution-distance from orifice have been plotted for each air pad shape. The results indicate that the rectangle air pad has the best pressure distribution.

Keywords: Air Bearing, Air Table, Air Pad, Pressure Distribution, Simulation, Ultra Precision Machine

Reference: Akhondzadeh, M. and Vahdati, M., "Simulation of Air Pad Shape on Pressure Distribution in Air Gap of Air Table in Ultra Precision Machine Tools", Int J of Advanced Design and Manufacturing Technology, Vol. 7/ No.1, 2014, pp. 27-33.

Biographical notes: M. Akhondzadeh received his MSc in Mechanical Engineering from University of K. N. Toosi University of Technology 2011. He is currently faculty member at the department of engineering, IAU Ahwaz Branch, Khuzestan, Iran. His current research interest includes Ultra Precision Machining and Nanomachining. **M. Vahdati** is Assistant professor of Mechanical Engineering at the K. N. Toosi University of Technology, Tehran,Iran. He received his PhD and MSc in manufacturing engineering from Utsunomiya University of Japan. His current research focuses on Ultra Precision Machining, Nanomachining, Abrasive Fluid Machining, etc.

1 INTRODUCTION

Increasing demand for precise manufacturing components for IT industries, electronics, nuclear energy, and defense has led to the appearance of ultra precision machining processes. Examples of these components are optical mirrors, computer memory discs, and drums for photocopying machines, all with surface finish in the nano-meter order and form accuracy of micron or sub-micron. This machine includes high precision motion mechanisms, in which spindles and tables move on a thin film of air, where the air film prevents metals from contact and decreases friction and heat generation. Also, it decreases vibration levels on work piece; thus fine surfaces can be achieved.

In order to eliminate vibration and other instabilities such as air hammer, especially in air tables, pressurized air before entering into air gap enters a pad. Instability depends on parameters such as pressurized air feeding method, orifice diameter, restriction method, air film thickness, pressure distribution in air gap, etc. Pressure distribution is one of key significant factors in air table vibration. The number of air pads, their shape, and size are among the critical parameters that affect pressure distribution too.

In this study, the effect of air pad shape on pressure distribution in air film have been analyzed using simulation method. Fig. 1 shows an air table with air pad.

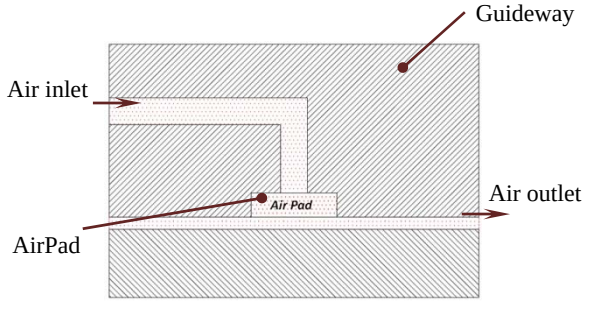

Fig. 1 Air table or guide way schematic

In 2002 Chen et al., investigated an arc type aerostatic grooved bearing [1]. He studied an aerostatic bearing with four axial and circumferential shallow grooves theoretically. He analyzed the effect of air film thickness in an investigation of pressure distribution in grooved and ungrooved bearings. In 2002 Chen and Lin presented a work on static behavior and dynamic stability analysis of grooved rectangular aerostatic thrust bearings, in which the studied air pads were in rectangle shape and had X-type grooves [2].

They analyzed these bearings theoretically and experimentally and reported similar results for pressure distribution in air gap. In 2010 Chen et al., analyzed a compound restrictor circular gas bearing with three straight and arc shallow grooves machine don the bearing surface, with supplied gas flow and reported same results for pressure distribution [3].

In 2009 Eleshaky analyzed pressure fallings in aerostatic circular thrust bearing by CFD method [4]. He simulated and computed different air film thickness for analyzing pressure falling in air film. In 2010 Miyatake and Yoshimoto presented numerical investigation on static and dynamic characteristics of aerostatic thrust bearing with small feed holes [5]. They have analyzed effects of small feed holes and their number on gas velocity, and damping factor, by using CFD capabilities of ANSYS.

In 2013 Akhondzadeh and Vahdati have investigated effect of size and number of rectangular air pockets on air spindle vibrations [6]. In their research air pockets with minimum number and size, have shown minimum vibration. In 2013, Akhondzadeh and Vahdati, also, investigated the effect of shape and depth of air pockets on air spindle vibration in ultra precision machining [7]. They expressed that the air spindle with rectangle shape of air pocket at low rotational speed have minimum vibration. In 2013, Akhondzadeh and Vahdati, investigated effects of shape, depth, size and number of air pockets on air spindle vibration altogether and performed 243 experiments [8].

2 AIR BEARING EQUATIONS

For an aerostatic journal bearing, as shown in Fig. 2(a), air is supplied from an externally pressure source and passes through entries with orifice compensation as shown in Fig. 2(b). Orifices are located double-rows about symmetry plane and evenly around the circumference of the bearing. Assuming the air as perfect gas which is compressible, isothermal and laminar, the non-dimensional Reynolds equation could be derived from Navier–Stokes and continuity equations. In the two dimensional Cartesian coordinates it may be shown as:

$$\frac{\partial}{\partial\theta}\left[\bar{h}^3\frac{\partial\bar{P}^2}{\partial\theta}\right]+\left(\frac{D}{L}\right)^2\frac{\partial}{\partial\bar{z}}\left[\bar{h}^3\frac{\partial\bar{P}^2}{\partial\bar{z}}\right]=2\Lambda\frac{\partial}{\partial\theta}\left(\bar{P}\bar{h}\right)+4\gamma\Lambda\frac{\partial(\bar{P}\bar{h})}{\partial\tau} \quad (1)$$

where D and L are bearing diameter and length, P and h are non-dimensional pressure and thickness of film, y and z are angular and axial coordinates of bearing, respectively, t is non-dimensional time, L is bearing number and g is whirl ratio.

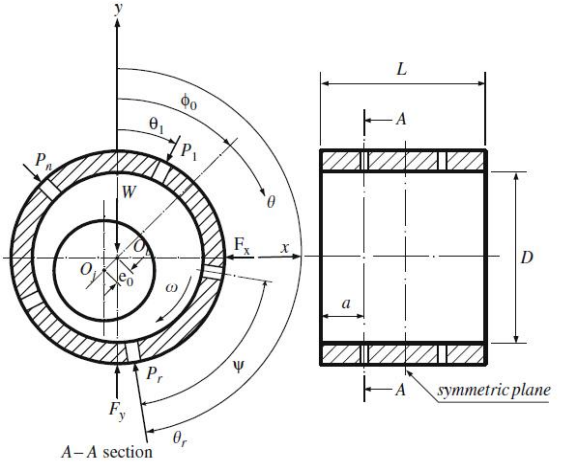

(a)

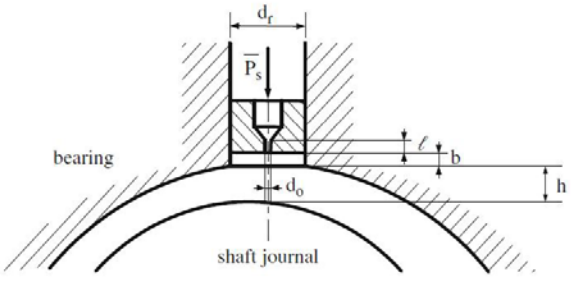

(b)

Fig. 2 Configurations of (a) an aerostatic bearing with double-array entries compensated by (b) orifice restriction

3 PROCEDURE

In order to study the effect of air pad shape on pressure distribution of air film, the FLUID142 element was used for simulation in FLOTRAN environment of ANSYS. The shapes that were selected for analyses, included triangle, rectangle, pentagon, hexagon, ellipse, and circle. The air pad area for all shapes was taken constant, equal to 314 mm^2, and depth of 3 mm. Fig. 3 shows one of the modelled air cells in ANSYS.

Air density and viscosity equals to 1.293 kg/mm^3 and 1.983×10^{-3} kg/ m.s, respectively. The free mode and size 3 was selected for meshing, where an elliptical meshed air pad is shown in Fig. 4.The pressure at input nozzle was set on 2 bars, and air velocity on all faces except input and output conditions were constrained zero. The air velocity at input face was selected equal to 10 m/s and pressure value at output faces loaded as 0 bars. A sample of constraints and loading on air table is presented in Fig. 5.

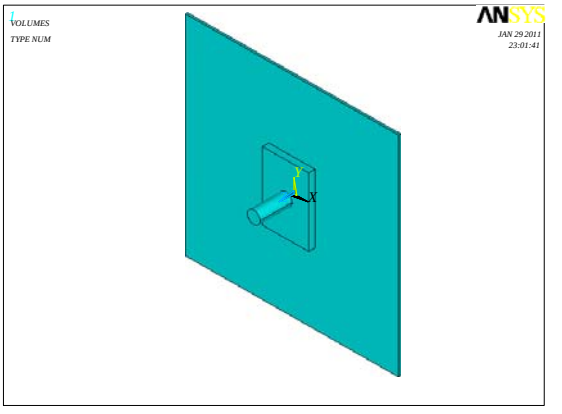

Fig. 3 Modeled air cell in ANSYS for rectangular air pad

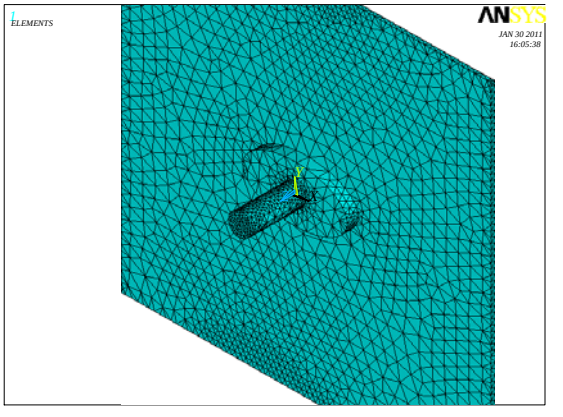

Fig. 4 Meshed air cell in ANSYS for elliptical air pad

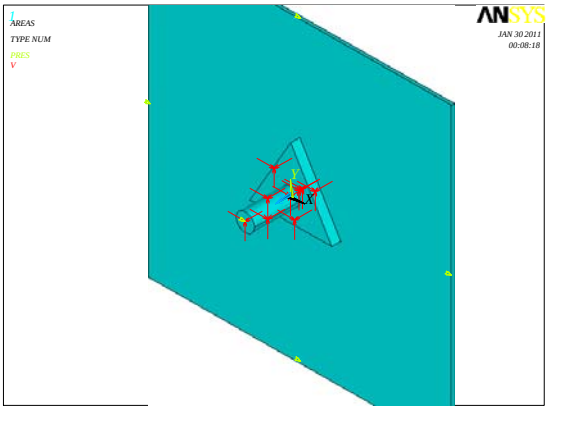

Fig. 5 Constraint and loading on air table for triangular air pad

4 RESULTS

Figs. 6 to 11 have shown air pressure distributions within entrance, body, and exit of the air pads for

various air pad geometries including triangle, rectangle, pentagon, hexagon, ellipse, and circle.

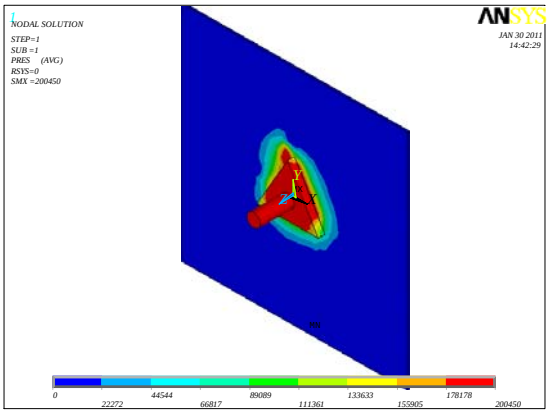

Fig. 6 Pressure distribution in air film for triangular air pad

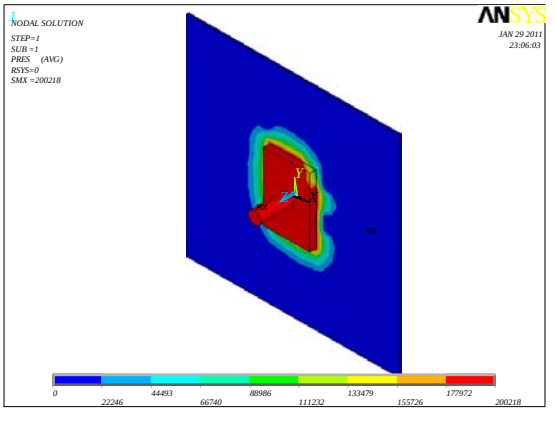

Fig. 7 Pressure distribution in air film for rectangularair pad

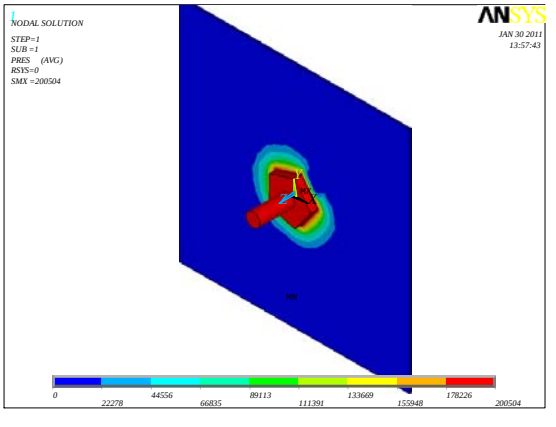

Fig. 8 Pressure distribution in air film for pentagonal air pad

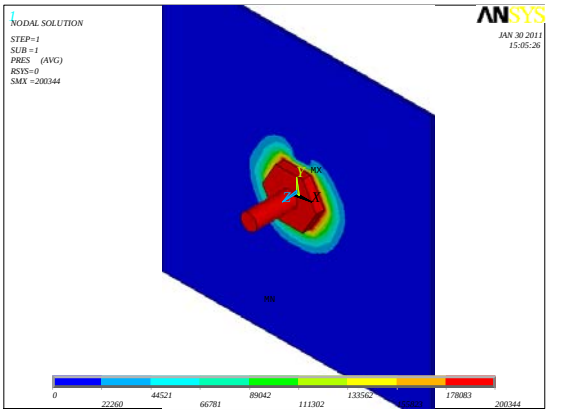

Fig. 9 Pressure distribution in air film for hexagonal air pad

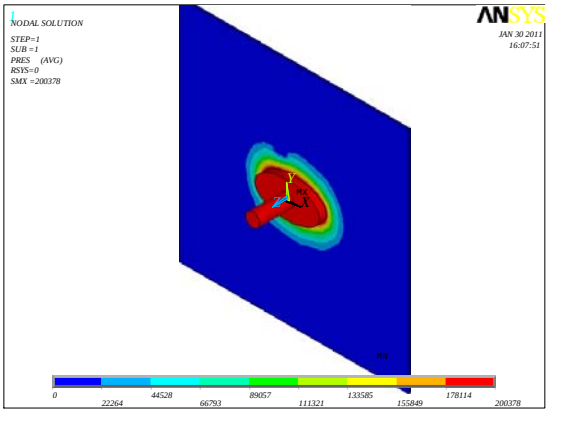

Fig. 10 Pressure distribution in air film for elliptical air pad

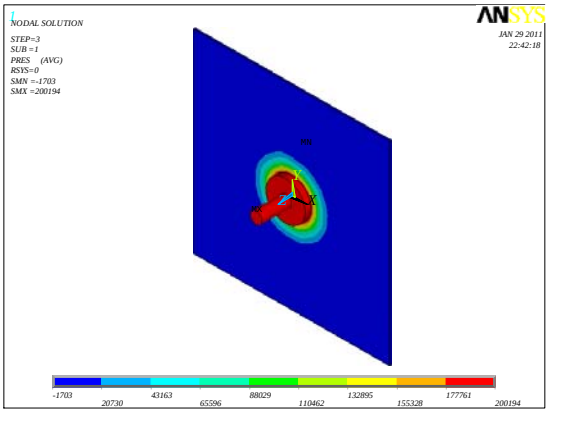

Fig. 11 Pressure distribution in air film for circular air pad

Also, pressure distribution versus distance from nozzle position graphs for various air pad geometries are shown in Figs. 12-17. In these Figs., the pressure distribution values versus distance from nozzle position are plotted for all elements.

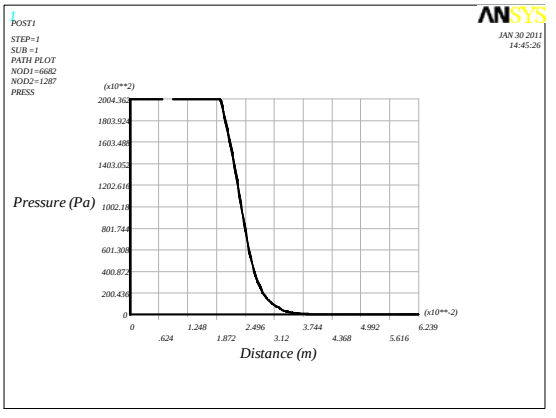

Fig. 12 Pressure distribution plot for triangular air pad

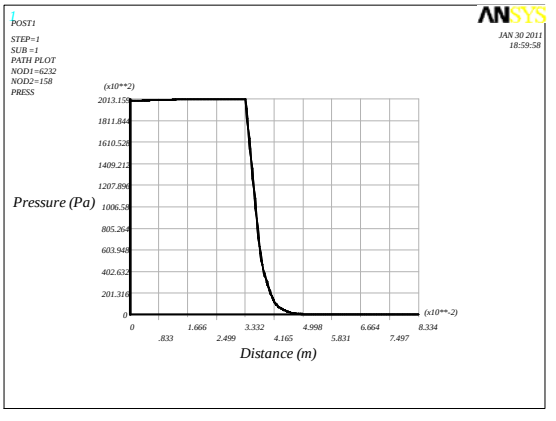

Fig. 13 Pressure distribution plot for rectangular air pad

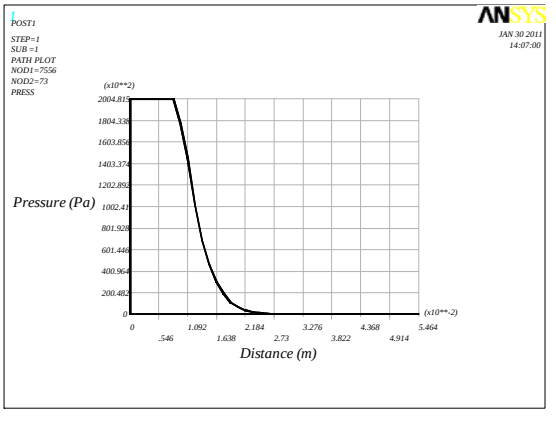

Fig. 14 Pressure distribution plot for pentagonal air pad

From Figs. 12 to 17 it may be found that pressure falling in air pads occurs at 1.945, 3.332, 0.819, 2.321, 2.669, and 1.240 cm from nozzle position for triangular, rectangular, pentagonal, hexagonal, elliptical and circular air pads, respectively; and achieve 0 value at 3.744, 4.998, 2.357, 3.798, 3.768, and 2.480 cm from nozzle position, respectively.

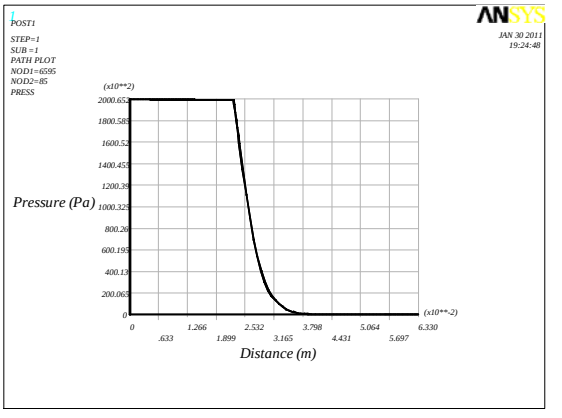

Fig. 15 Pressure distribution plot for hexagonal air pad

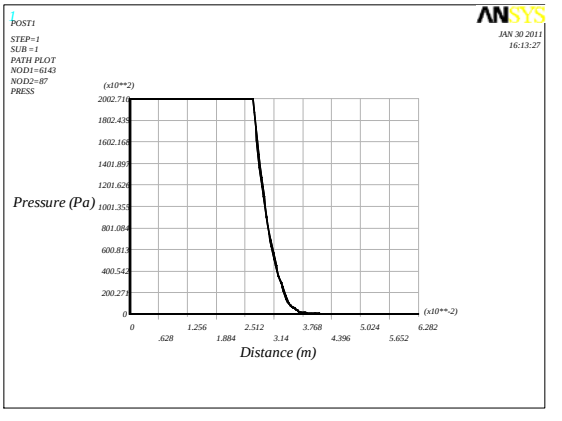

Fig. 16 Pressure distribution plot for elliptical air pad

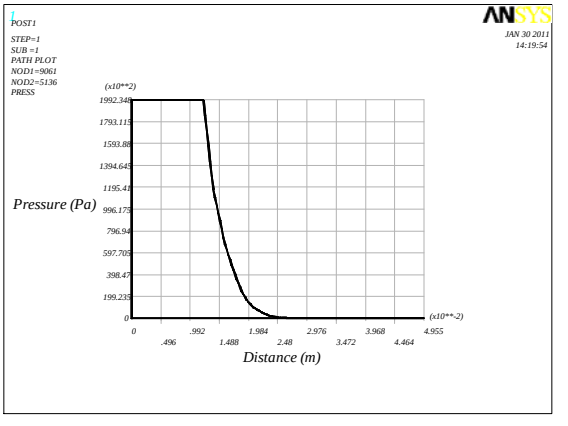

Fig. 17 Pressure distribution plot for circular air pad

Fig. 18 shows experimental results reported by [6]. Effect of 3 air pad geometries (1) triangle (2) rectangle, and (3) circle on air spindle vibrations are plotted in this graph, in which the air spindle with rectangular air pads have shown minimum vibration. It is noted that pressure distribution in air film is one of the most significant factors in air spindle vibrations.

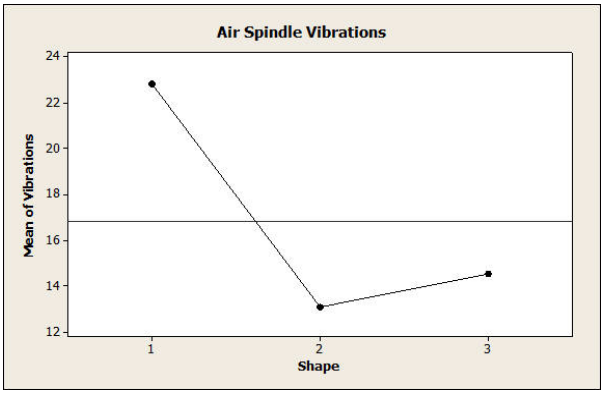

Fig. 18 Plot of air pad geometries on air spindle vibrations

5 CONCLUSION

1. Air table have direct effects on machined surface roughness; for this reason, in order to achieve very smooth surfaces, with nano-meter resolutions, studying the air table becomes vitally important.
2. In this study, effect of air pad on pressure distribution was simulated three dimensionally; therefore, the potentials of air pad geometry on pressure distribution analyses were evaluated.
3. According to the pressure distribution plots, rectangular air pad has lower pressure falling from feed hole. Therefore, this geometry has suitable pressure distribution with respect to others.
4. Also, from pressure distribution plots, pentagonal air pad has higher pressure falling from feed hole position and for air table reasons isn't suitable.
5. Comparing the results from [8] and the simulation results, it may be seen that there is an acceptably good agreement between these results. Moreover, the rectangular air pad provides good pressure distribution and vibration.

6 NOMENCLATURE

a	land width of axial flow (m)
b	pocket depth
C	radial clearance of bearing (m)
D	diameter of bearing (m)
d_o	diameter of orifice (m)
d_r	inlet diameter
e_0	steady-state eccentricity
F_x, F_y	force components (N) due to air film in the x and y directions
h, $\bar{h}$	film thickness (m), $\bar{h} = {h}/{c}$
L	axial length of bearing (m)
L	supply orifice length (m)
O_b, O_j	bearing center, spindle or journal center
$\bar{P}$	non-dimensional pressure
P_a	atmospheric pressure (N/m^2)
P_1, P_r, P_n	pressure at the 1st, *r*th and *n*th inlet (N/m^2)
P_s, $\bar{P}_s$	supply pressure (N/m2), $\bar{P}_s = {P_s}/{P_a}$
t	time (sec)
W	load capacity(N)
x, y	Cartesian coordinates of air film
z, $\bar{z}$	axial coordinate of bearing, $\bar{z} = {z}/{(L/D)}$
Λ	bearing number,$\Lambda = {6\mu\omega}/{P_a(C/R)^2}$
Ω	whirl frequency of journal center about the equilibrium axis
ψ	circumferential angle between adjacent restrictions, $\psi = {2\pi}/{n}$
ϕ_o	steady-state attitude angle
μ	dynamic viscosity of air (Ns/m^2)
θ	angular coordinate, $\theta = {x}/{R}$
θ_r	circumferential position of the *r*th feeding hole
τ	non-dimensional time, $\tau = \Omega t$
ω	spindle speed (rad/s)
γ	whirl ratio

REFERENCES

[1] Chen, M. F., Chen, Y. P., and Lin, C. D.;"Research on the arc type aerostatic bearing for a PCB drilling station"; Tribology International, Vol. 35, 2002, pp. 235-243.
[2] Chen, M. F., Lin, Y. T.;"Static behavior and dynamic stability analysis of grooved rectangular aerostatic thrust bearings by modified resistance network

method"; Tribology International, Vol. 35, 2002, pp. 329-338.

[3] Chen, M. F., Huang, W. L., and Chen, Y. P.; "Design of the aerostatic linear guide way with a passive disk-spring compensator for PCB drilling machine"; Tribology International, Vol. 43, 2010, pp. 395-403.

[4] Mohamed E. Eleshaky, "CFD investigation of pressure depressions in aerostatic circular thrust bearing", Tribology International, Vol. 42, 2009, pp. 1108-1117.

[5] Miyatake, M., Yoshimoto, S., "Numerical investigation of static and dynamic characteristics of aerostatic thrust bearing with small feed holes", Tribology International, Vol. 43, 2010, pp. 1353-1359.

[6] Akhondzadeh, M., Vahdati, M., "Experimental Investigation on Effect of Number and Size of Rectangular Air Pockets on Air Spindle Vibrations in Nanomachining", Proc IMech E Part B: Journal of Engineering Manufacture, 2013, Vol. 227, No. 2, pp. 281-285.

[7] Akhondzadeh, M., Vahdati, M., "An experiment on the Shape and Depth of Air Pocket on Air Spindle Vibrations in Ultra Precision Machine Tools", Proc IMech E Part B: Journal of Engineering Manufacture, 2013, Vol. 227, No. 4, pp. 616-620.

[8] Akhondzadeh, M., Vahdati, M., "Air Pocket Effects on Air Spindle Vibrations in Nanomachining", Proc IMech E Part B: Journal of Engineering Manufacture, 2014, Vol. 228, No. 3, pp. 328-336.